GEOPHYSICAL RESEARCH LETTERS, VOL. 35, L16315, doi:10.1029/2008GL034769, 2008

A new finite-frequency shear-velocity model of the European-Mediterranean region

D. Peter,[1] L. Boschi,[1] F. Deschamps,[1] B. Fry,[1] G. Ekström,[2] and D. Giardini[1]

Received 22 May 2008; revised 21 July 2008; accepted 25 July 2008; published 30 August 2008.

[1] We invert a global phase-anomaly database of intermediate- to long-period Rayleigh waves, recently updated with increased coverage in the European-Mediterranean region, on a global scale with a higher resolution parameterization in the region of interest. We first compare phase-velocity inversions based on ray and finite-frequency theory and derive for each a corresponding set of local phase-velocity dispersion curves (one per model pixel) between 35 s to 300 s period. Effects of the two different theories on the three-dimensional upper-mantle structure are investigated by inverting each dispersion curve for radial shear-velocity profiles. The combination of a gradient-descent method and a random-Monte-Carlo model search provides an estimated shear-velocity model with associated uncertainties for depths between 40 km to 400 km. While differences between ray-theoretical and finite-frequency models are small compared to model uncertainty, comparisons with independent models favor the finite-frequency one. **Citation:** Peter, D., L. Boschi, F. Deschamps, B. Fry, G. Ekström, and D. Giardini (2008), A new finite-frequency shear-velocity model of the European-Mediterranean region, *Geophys. Res. Lett.*, *35*, L16315, doi:10.1029/2008GL034769.

1. Introduction

[2] In view of current plans to build a European seismological reference model [*Ritzwoller et al.*, 2006], a new surface-wave dataset was assembled [*Fry et al.*, 2008], achieving unprecedentedly dense coverage of the continent. The dataset combines global and regional observations, which helps to further constrain regional seismic models [see, e.g., *Shapiro and Ritzwoller*, 2002]. Tectonics in Europe and in the Mediterranean region are governed by a complex interaction of the African, Eurasian and Arabian plates, comprehensively investigated in several tomographic studies [*Spakman et al.*, 1993; *Wortel and Spakman*, 2001; *Piromallo and Morelli*, 2003; *Boschi et al.*, 2004; *Marone et al.*, 2004; *Fry*, 2007; *Schmid et al.*, 2008]. Recent phase-velocity models of the region, found using analytical finite-frequency sensitivity kernels, show some significant discrepancies with ray-theoretical ones, especially between the Southern Apennines and the Hellenic Arc [*Fry et al.*, 2008].

[3] It is unclear how such differences in phase-velocity distributions reflect differences in the underlying seismic structures. Identifying a one-dimensional seismic velocity profile from a local dispersion curve is a nonlinear, non-unique problem [*Knopoff*, 1972]. An exploration of the solution space more thorough than those afforded by linearized inversions becomes therefore necessary, to identify a most likely seismic profile and estimate its uniqueness. Focusing on the well sampled European-Mediterranean region [*Fry et al.*, 2008], we use Rayleigh-wave phase-velocity maps derived by both ray and numerical finite-frequency theory [*Peter et al.*, 2007] to build a new set of dispersion curves which, in a second step, are inverted for radial V_s (shear velocity) profiles. We then compare the resulting three-dimensional shear-velocity models with earlier studies of the region's seismic structure.

2. Data

[4] The global dispersion database of *Ekström et al.* [1997], updated by *Boschi and Ekström* [2002], was further expanded by *Fry* [2007], applying the same measurement technique as *Ekström et al.* [1997] to recordings of both Love and Rayleigh waves from MidSEA, SDSNet, TomoCH and GRSN stations [see *Fry et al.*, 2008, and references therein]. This results in a particularly dense coverage over Europe and the Mediterranean Basin. We invert a total of 677,234 measurements of Rayleigh waves at all available periods between 35 s and 300 s and epicentral distances between 15° and 165°, and for both minor and major arcs.

3. Method

[5] We invert for local phase velocities with a global multiple-resolution parameterization, where Europe and the Mediterranean region are parameterized with blocks of approximately equal size of 1° × 1°, everywhere else by 3° × 3° blocks. At each period from 35 s to 300 s, we use a least-squares algorithm [*Paige and Saunders*, 1982] to find a phase-velocity map derived by both ray- and finite-frequency theory. For the latter, we computed sensitivity kernels entirely numerically as described and illustrated by *Peter et al.* [2007], in the assumption that the Earth structure be relatively smooth. Our choice of solution is based on an analysis of the L-curves after deriving sets of solution models with different strength of the smoothness damping constraint (no other regularization was applied). For each theory, we compare the inversion solutions corresponding to points of equal curvature on the L-curve [*Peter et al.*, 2007].

[6] Dispersion curves derived from these phase-velocity maps are assembled for each inversion pixel within Europe and the Mediterranean region (900 locations total). At each pixel, we next invert the corresponding dispersion curve to find V_s in six distinct layers (40–60 km, 60–100 km, 100–

[1]Institute of Geophysics, ETH Zurich, Zurich, Switzerland.
[2]Lamont-Doherty Earth Observatory, Earth Institute at Columbia University, Palisades, New York, USA.

0094-8276/08/2008GL034769$05.00

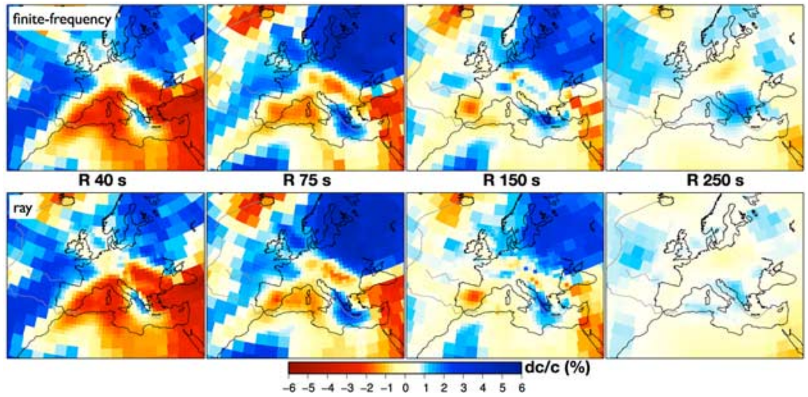

Figure 1. Phase-velocity maps obtained from inversions based on numerical finite-frequency (top) and ray theory (bottom), from *Fry et al.* [2008] measurements at 40 s, 75 s, 150 s and 250 s.

150 km, 150–220 km, 220–310 km and 310–400 km). In the assumption of a perfectly elastic upper mantle (i.e., neglect of attenuation), we use Knopoff's method [*Schwab and Knopoff*, 1970], to calculate a synthetic dispersion curve for each seismic profile generated by our search algorithm. The search algorithm consists of a gradient-descent inversion [*Tarantola*, 2005] subsequently refined by a Monte-Carlo search.

[7] The starting seismic profile combines PREM [*Dziewonski and Anderson*, 1981] vertically polarized V_s, compressional velocity V_p, and density for the mantle together with a crustal description from Crust-2.0 [*Bassin et al.*, 2000], where ocean and Moho depths have been interpolated from the more detailed ones given in the European crustal model EuCrust-07 [*Tesauro et al.*, 2008].

[8] In the Monte-Carlo refinement, we generate $\sim 10^5$ radial profiles by randomly perturbing the values of V_s at each layer up to 10%, while keeping density and P-velocity fixed [*Deschamps et al.*, 2008]. Limited to some locations, we verified that even after increasing the number of sampled solutions to $\sim 10^7$, our final result remains stable.

[9] Our cost function χ^2, accounting for the observational error σ_j (estimated by *Ekström et al.* [1997] and converted to phase velocity) at each period T_j and for the difference between "observed" $c_{obs}(T_j)$ and computed $c(T_j)$ phase-velocity, is defined as:

$$\chi^2 = \sum_j \frac{\left[c_{obs}(T_j) - c(T_j)\right]^2}{\sigma_j^2} + \eta \sum_j \frac{\left[c'_{obs}(T_j) - c'(T_j)\right]^2}{\sigma_j^2},$$

where $'$ denotes derivation with respect to period and η acts as a weighting parameter for the second term, chosen so that the shapes and offsets of the dispersion curves are fit equally well. For all solution profiles for which the phase-velocities lie within one standard deviation of the observational error, we calculate a probability p that depends on the corresponding χ^2 value:

$$p = k\ e^{-\frac{\chi^2}{2}}$$

where k is a normalization constant. Our final preferred profile coincides with the weighted (with weight p) average of all those profiles, accompanied by the corresponding standard deviations [*Deschamps et al.*, 2008].

4. Results

[10] Figure 1 shows examples of our phase-velocity maps at four different periods (40 s, 75 s, 150 s and 250 s) with important discrepancies between ray- and finite-frequency-theory-derived maps visible for longer periods at 150 s and 250 s [*Fry et al.*, 2008]. Although the sensitivity of Rayleigh waves at the shortest period we consider (35 s) has highest sensitivity mostly below the Moho [*Boschi and Ekström*, 2002], their sensitivity to the crust is still considerable. We constructed an artificial V_s profile, with crustal layers derived from Crust-2.0 and EuCrust-07 but an artificial upper mantle, and computed a corresponding "synthetic" dispersion curve by Knopoff's method. We then inverted this synthetic dispersion curve with starting profiles different from the original "input" model. Figure 2a illustrates results of two such tests with crustal structure fixed either to PREM crust or to our crustal model based on Crust-2.0 and EuCrust-07 (as was used to generate the synthetics). It is clear that (i) even if the starting model for the inversion is very wrong (gray dashed line) the input model can be retrieved properly, but (ii) only if the crustal model is reliable. In the absence of an accurate crustal model, retrieved upper-mantle structure is dubious down to ~200 km depth.

[11] The three-dimensional models derived by ray and finite-frequency theory exhibit differences under Southern Italy and the Hellenic arc at depths between 150–400 km. Figure 2b shows one of the V_s profiles from the "observed" dispersion curves derived by finite-frequency or ray theory for a location in Southern Italy (41.5°N, 16.5°E). In both cases, crustal structure is fixed to our crustal model based on Crust-2.0 and EuCrust-07. Between 60 km and 100 km, both models show a positive anomaly, which at 100–150 km changes to a low-velocity layer. The inversion of the finite-frequency dispersion curve shows higher anomalies at depths between 150–310 km. Figures 3 and 4 combine all the V_s perturbations (and their standard deviations) found as described. Standard deviations grow with depth and vary up

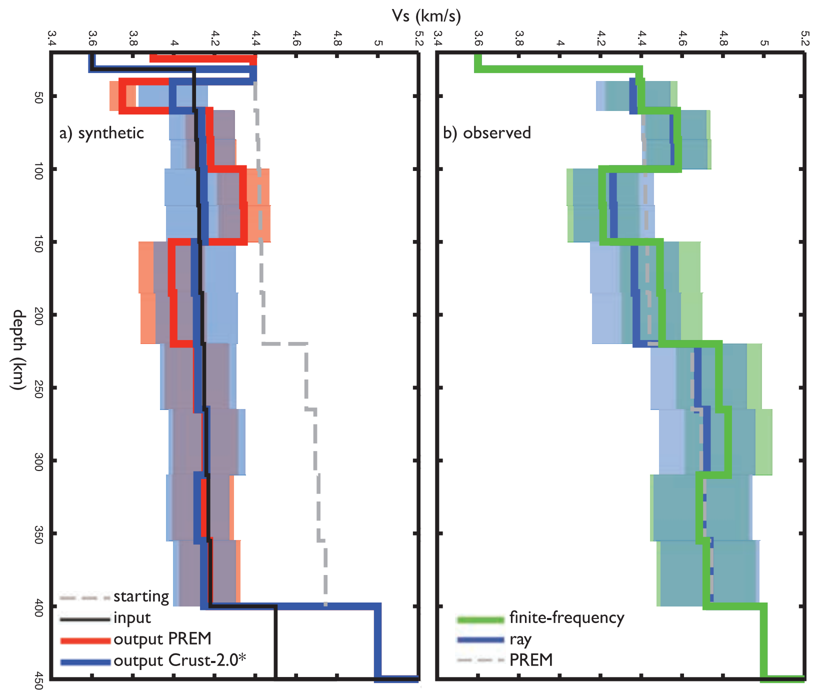

Figure 2. Local V_s profiles and their standard deviations (shaded areas). (a) Inversions from a "synthetic" dispersion curve computed from an artificial "input" profile (black line). Output profiles are obtained from a starting model with an upper-mantle PREM profile (gray dashed) and crustal structure fixed to either PREM (red) or the same crustal model used as input (blue). (b) Inversions from dispersion curves obtained from finite-frequency (green) and ray-theory (blue) maps (Figure 1) for a location in Southern Italy. The starting profile consists of a PREM mantle and crustal structure fixed to a combined Crust-2.0- and EuCrust-07-based model.

to 6%, which indicates a decreased resolving power in the dispersion curves.

5. Discussion

[12] Comparisons between our ray-theoretical and finite-frequency results confirm the important differences pointed out by *Fry et al.* [2008]. At the longest periods, our finite-frequency maps exhibit stronger anomalies than those derived by *Fry et al.* [2008] via analytical finite-frequency kernels. We additionally find that the crustal structure plays an important role in the correct determination of the uppermost ~200 km of the radial V_s profiles, confirming the findings of *Waldhauser et al.* [2002]. Including shorter

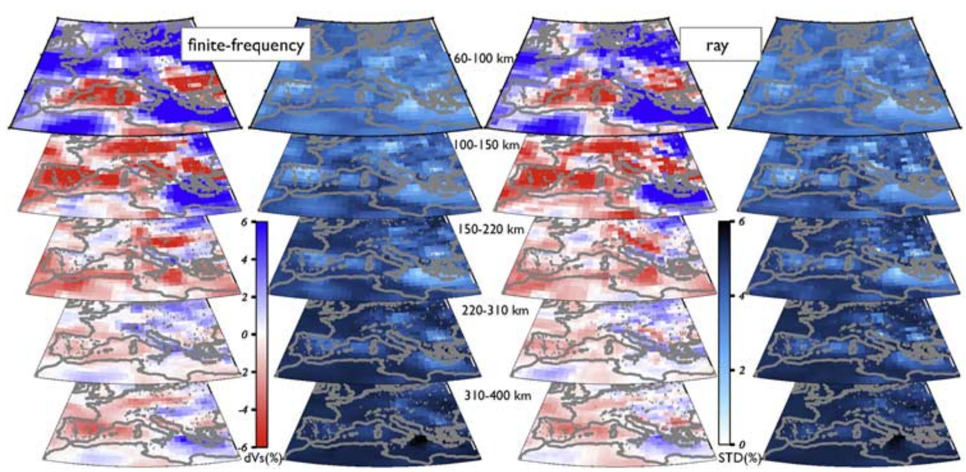

Figure 3. V_s perturbations (dVs) with respect to PREM at 60–100 km, 100–150 km, 150–220 km, 220–310 km and 310–400 km depths based either on finite-frequency (left) or ray-theoretically (right) derived dispersion curves. The standard deviations (STD) of the corresponding shear-velocity anomalies are given to the left of the models.

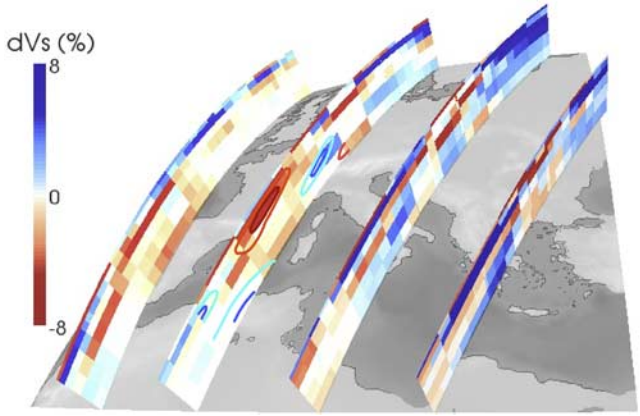

Figure 4. Perspective view of four different cross-sections through the finite-frequency shear-velocity model of Figure 3. The Tunisia-Central Europe cross-section also shows contour lines from the model of *Boschi et al.* [2004].

surface-wave periods from noise correlations could allow us to extend our model search and invert simultaneously for crustal layer parameters [*Panza et al.*, 2007]. In both V_s-models (Figure 3) we find the same prominent features as *Boschi et al.* [2004] and *Marone et al.* [2004]. Although our models show a strong, high-velocity anomaly under the Hellenic Arc at 60–150 km depths, related to the Dinarides-Hellenides subduction, the dip angle is only poorly resolved. At 220–310 km depth, a high V_s-anomaly stretching along the Southern Apennines up to Northern Italy is identified in the finite-frequency inversion, while in the ray-theoretical model this anomaly seems to be shifted eastwards under the Adriatic sea.

[13] Our estimated model error (Figure 2) is between 2% to 6%, obscuring most ray-theory vs. finite-frequency discrepancies. Yet, error estimates from *Ekström et al.* [1997] are conservative, and there are suggestive hints that the finite-frequency method is indeed enhancing resolution. With respect to the ray-theory solution, the finite-frequency one is more coherent with V_p structure found in a tectonic reconstruction of the temperature field [*de Jonge et al.*, 1994]: compare, e.g., Figure 3 (layer at 220–310 km) with Figure 6 of *Boschi et al.* [2004]. In the same depth range, a fast anomaly under the Central Alps, associated with past subduction, also found by *Schmid et al.* [2008], is reproduced more clearly in our finite-frequency model than in the ray-theoretical one: compare, in particular, our Tunisia-Central Europe cross-section of Figure 4 with Figure 8 of *Boschi et al.* [2004].

6. Conclusions

[14] We inverted a new phase-anomaly database [*Fry et al.*, 2008] of intermediate to long-period Rayleigh waves, confirming (at 150 s period) the presence of a distinct high-phase-velocity zone between Southern Italy and the Hellenic Trench in finite-frequency inversions, which is shifted to the Balkan coastline for ray-theoretical inversions. We constructed three-dimensional shear-velocity models by inverting dispersion curves, found at each location in the European-Mediterranean region, from the previously obtained phase-velocity maps derived by ray- and finite-frequency theory. In general, differences are small compared to a conservative estimate of model error, but a tectonic reconstruction [*de Jonge et al.*, 1994] of the region's temperature field supports our finite-frequency model. Including dispersion measurements at shorter wave periods and basing the inversion on refined models of the crust will allow to reduce the error bar on tomographic results, and eventually quantify the improvement achieved via the finite-frequency approach.

[15] **Acknowledgments.** We thank John Woodhouse for giving us access to the large computational facility at the Department of Earth Sciences, Oxford University. We also gratefully acknowledge support from the European Commission's Human Resources and Mobility Programme, Marie Curie Research Training Networks.

References

Bassin, C., G. Laske, and G. Masters (2000), The current limits of resolution for surface wave tomography in North America, *Eos Trans. American Geophysical Union*, *81*(48), Fall Meet. Suppl., Abstract S12A-03.
Boschi, L., and G. Ekström (2002), New images of the Earth's upper mantle from measurements of surface wave phase velocity anomalies, *J. Geophys. Res.*, *107*(B4), 2059, doi:10.1029/2000JB000059.
Boschi, L., G. Ekström, and B. Kustowski (2004), Multiple resolution surface wave tomography: The Mediterranean basin, *Geophys. J. Int.*, *157*, 293–304.
de Jonge, M. R., M. J. R. Wortel, and W. Spakman (1994), Regional scale tectonic evolution and the seismic velocity structure of the lithosphere and upper mantle: The Mediterranean region, *J. Geophys. Res.*, *99*, 12,091–12,108.
Deschamps, F., S. Lebedev, T. Meier, and J. Trampert (2008), Stratified seismic anisotropy reveals past and present deformation beneath the east-central United States, *Earth Planet. Sci. Lett.*, in press.
Dziewonski, A. M., and D. L. Anderson (1981), Preliminary reference Earth model, *Phys. Earth Planet. Inter.*, *25*, 297–356.
Ekström, G., J. Tromp, and E. W. F. Larson (1997), Measurements and global models of surface wave propagation, *J. Geophys. Res.*, *102*, 8137–8157.
Fry, B. (2007), Surface wave tomography of the Mediterranean and central Europe: A new shear wave velocity model, Ph.D. thesis, ETH Zurich, Zurich, Switzerland.
Fry, B., L. Boschi, G. Ekström, and D. Giardini (2008), Europe-Mediterranean tomography: High correlation between new seismic data and independent geophysical observables, *Geophys. Res. Lett.*, *35*, L04301, doi:10.1029/2007GL031519.
Knopoff, L. (1972), Observation and inversion of surface-wave dispersion, *Tectonophysics*, *13*(1–4), 497–519.
Marone, F., S. van der Lee, and D. Giardini (2004), Three-dimensional upper-mantle S-velocity model for the Eurasia-Africa plate boundary region, *Geophys. J. Int.*, *158*, 109–130.
Paige, C. C., and M. A. Saunders (1982), LSQR—An algorithm for sparse linear-equations and sparse least-squares, *Trans. Math. Software*, *8*, 43–71.
Panza, G. F., A. Peccerillo, A. Aoudia, and B. Farina (2007), Geophysical and petrological modelling of the structure and composition of the crust and upper mantle in complex geodynamic settings: The Tyrrhenian Sea and surroundings, *Earth Sci. Rev.*, *80*, 1–46.
Peter, D., C. Tape, L. Boschi, and J. H. Woodhouse (2007), Surface wave tomography: Global membrane waves and adjoint methods, *Geophys. J. Int.*, *171*, 1098–1117.
Piromallo, C., and A. Morelli (2003), P wave tomography of the mantle under the Alpine-Mediterranean area, *J. Geophys. Res.*, *108*(B2), 2065, doi:10.1029/2002JB001757.
Ritzwoller, M. H., Y. Yang, A. L. Levshin, R. Engdahl, and N. M. Shapiro (2006), Thoughts on a European seismic reference model: The role of surface waves from earthquakes and ambient noise, *Geophys. Res. Abstr.*, *8*, EGU06-A-05,281.
Schmid, C., S. van der Lee, J. C. VanDecar, E. R. Engdahl, and D. Giardini (2008), Three-dimensional S velocity of the mantle in the Africa-Eurasia plate boundary region from phase arrival times and regional waveforms, *J. Geophys. Res.*, *113*, B03306, doi:10.1029/2005JB004193.
Schwab, F., and L. Knopoff (1970), Surface-wave dispersion computations, Bull, *Seismol. Soc. Am.*, *60*, 321–344.
Shapiro, N. M., and M. H. Ritzwoller (2002), Monte-Carlo inversion for a global shear-velocity model of the crust and upper mantle, *Geophys. J. Int.*, *151*, 88–105.

Spakman, W., S. van der Lee, and R. van der Hilst (1993), Travel-time tomography of the European Mediterranean mantle down to 1400 km, *Phys. Earth Planet. Inter.*, *79*, 3–74.

Tarantola, A. (2005), *Inverse Problem Theory and Methods for Model Parameter Estimation*, Soc. for Ind. and Appl. Math., Philadelphia, Pa.

Tesauro, M., M. K. Kaban, and S. A. P. L. Cloetingh (2008), EuCRUST-07: A new reference model for the European crust, *Geophys. Res. Lett.*, *35*, L05313, doi:10.1029/2007GL032244.

Waldhauser, F., R. Lippitsch, E. Kissling, and J. Ansorge (2002), High-resolution teleseismic tomography of upper-mantle structure using an a priori three-dimensional crustal model, *Geophys. J. Int.*, *150*, 403–414.

Wortel, M. J. R., and W. Spakman (2001), Subduction and slab detachment in the Mediterranean-Carpathian region, *Science*, *291*(5503), 437–437.

L. Boschi, F. Deschamps, B. Fry, D. Giardini, and D. Peter, Institute of Geophysics, ETH Zurich, CH-8093 Zurich, Switzerland. (dpeter@erdw.ethz.ch)

G. Ekström, Lamont-Doherty Earth Observatory, Earth Institute at Columbia University, Palisades, NY 10964, USA.